

ANALYTICAL FORMULATION OF THE SINGLE-VISIT COMPLETENESS JOINT PROBABILITY DENSITY FUNCTION

DANIEL GARRETT AND DMITRY SAVRANSKY¹

Sibley School of Mechanical and Aerospace Engineering, Cornell University, Ithaca, NY 14853

¹Carl Sagan Institute, Cornell University, Ithaca, NY 14853

ABSTRACT

We derive an exact formulation of the multivariate integral representing the single-visit obscurational and photometric completeness joint probability density function for arbitrary distributions for planetary parameters. We present a derivation of the region of nonzero values of this function which extends previous work, and discuss time and computational complexity costs and benefits of the method. We present a working implementation, and demonstrate excellent agreement between this approach and Monte Carlo simulation results.

Keywords: methods: analytical — methods: statistical — planetary systems — planets
and satellites: detection — techniques: high angular resolution

1. INTRODUCTION

Obscurational completeness was introduced by [Brown \(2004b\)](#) as a necessary, but not sufficient, condition for detection of an exoplanet. Assuming distributions for semimajor axis and eccentricity of planetary orbits, Brown defined obscurational completeness as the probability of a planet falling

outside a telescope’s central obscuration, thus becoming potentially observable. This concept was expanded (Brown 2005) to include selection effects due to photometric restrictions on exoplanet observability introduced by telescope optics. Completeness can be extended to indirect exoplanet detection methods like reflex astrometry (Brown 2009a) and account for successive observations (Brown & Soummer 2010). Benefits of completeness studies include realistic expectations of mission outcomes based on objective terms for search power and a scientific metric to inform and optimize mission designs (Brown 2009b). These studies have been used in mission analysis and design for a variety of proposed exoplanet observatories (Brown 2009a; Lindler 2007; Savransky & Kasdin 2008; Savransky et al. 2010; Savransky 2013; Stark et al. 2014; Brown 2015; Stark et al. 2015).

Single-visit completeness is determined by the assumption that an exoplanet is observable if its angular separation from its star is greater than the observatory’s inner working angle (IWA) and less than the observatory’s outer working angle (OWA) while also being illuminated such that the difference in brightness between the star and planet (Δmag) is below a limiting value (Δmag_0). The IWA and OWA represent the minimum and maximum angular separation of the field of view. Δmag_0 is where unresolvable confusion between the planet signal and noise occur.

For simple cases an analytic functional representation of completeness may be possible. With the exception of Agol (2007), previous approaches to calculating completeness have relied on Monte Carlo trials because of the complexity of the assumed distributions. Probability distributions are assumed for the orbital elements and physical properties necessary for determining separation and Δmag . A large, equal number of samples (Brown (2005) used 100 million) is generated from each of the distributions. Successive function evaluations are made, including solving Kepler’s equation iteratively, leading to the calculation of star-planet separation and Δmag for each set of samples. A two-dimensional histogram of these values is constructed which gives the expectation, or relative frequency of occurrence, of separation and Δmag for each bin of the two-dimensional histogram.

Dividing the expectation values by the area of each bin gives the joint probability density function. Integrating with respect to separation and Δmag over this joint probability density function yields a cumulative density function which gives the completeness, or probability that an observatory with given Δmag_0 , IWA, and OWA, observing a specific star for the first time, will detect a planet belonging to the assumed population.

The Monte Carlo trial approach of finding the expectation is analogous to numerical integration. Increasing the number of samples, n , in the Monte Carlo trial approach results in reduced error which goes as $O(n^{-1/2})$ (Davis & Rabinowitz 2007). To reduce the error by one decimal place, the number of samples must be increased by a factor of 100. For one-dimensional numerical integration, the simple Riemann sum, $O(n^{-1})$; Newton-Cotes quadrature, better than $O(n^{-2})$; or Gaussian quadrature all have better error performance for n sample points than Monte Carlo integration. Multidimensional integrals may be numerically integrated using a composition of one-dimensional integrals or product rules which will also have better error performance than Monte Carlo integration.

In terms of time complexity, the Monte Carlo trial approach requires sampling of quantities, solving Kepler's equation iteratively, additional function evaluations to get separation and Δmag , and sorting these values into a two-dimensional histogram. All of these operations can be performed in polynomial time or better. Numerical integration algorithms require functional evaluations at sample points, determination of weights, multiplying the weights with functional evaluations, and summing these values. All of these operations can be performed in polynomial time. Increasing the dimension of an integral exponentially increases the number of samples required which increases the computational time. Multidimensional integrals higher than about dimension three are better computed using Monte Carlo integration due to the computational time.

The bivariate distribution sampled by Monte Carlo trials is a function of non-independent variables. The completeness distribution must be sampled fully to find any one point of the joint probability

distribution accurately. Because of the number of parameters involved and the potential wide range of values these parameters may take, full sampling requires a large number of Monte Carlo trials. Increasing numbers of Monte Carlo trials increases the computational time of accurately determining completeness. For exoplanet mission simulators, it is desirable to produce completeness values quickly without sacrificing accuracy. Numerical integration of lower dimensional integrals would require fewer sample points and give better error and computational time performance for a single point of the joint probability density function.

We present a functional approach to determining single-visit completeness which avoids the under-sampling problem inherent in the Monte Carlo simulation. This approach also allows for calculation of a single point of the completeness joint probability density function without simulation of the entire phase space. We begin by presenting the necessary assumptions which allow the description of completeness in functional terms. These functional expressions are made to be as general as possible. We then discuss computational considerations of this approach and provide comparisons to the Monte Carlo trial approach.

2. ASSUMPTIONS

[Savransky et al. \(2011\)](#) presented a derivation of probability density functions for orbital parameters and observed quantities related to completeness under the following four assumptions:

1. Closed Keplerian orbits with negative specific orbital energy approximate planetary orbits
2. Orbital poles are uniformly distributed on the celestial sphere
3. Effects due to planet-planet interactions, such as resonant orbits, are ignored
4. Distance from the observer to the target star is much larger than the distance from the target star to any of its planets

These assumptions allow the description of each orbit with the parameter set $(a, e, \psi, \theta, \phi)$, where a is the semimajor axis, e is the eccentricity, and ψ, θ, ϕ are Euler angles determining the orientation of the orbit in the observer's reference frame. The true anomaly, ν , gives the position of the planet on its orbit at the time of observation. We will use these same assumptions and their following results to derive the joint probability density function for completeness.

A functional description of the apparent planet-star separation, s , and difference in brightness between the star and planet, Δmag , are required to derive the completeness joint probability density function. The first and third assumptions result in the familiar Keplerian distance between planet and star,

$$r = \frac{a(1 - e^2)}{1 + e \cos \nu}. \quad (1)$$

The fourth assumption results in an approximation of the star-planet-observer or phase angle β giving the apparent planet-star separation as

$$s = r \sin \beta. \quad (2)$$

[Brown \(2005\)](#) defined the ratio of fluxes between planet and star as

$$F_R \triangleq \frac{F_p}{F_s} = p \Phi(\beta) \left(\frac{R}{r} \right)^2, \quad (3)$$

where p and R are the planet's geometric albedo and radius and Φ is the planet's phase function. The difference in brightness between the star and its planet is given by

$$\Delta\text{mag} = -2.5 \log_{10} F_R. \quad (4)$$

Equations (2), (3), and (4) give the relations between the variables (p, R, β, r) required for deriving a functional expression for the completeness joint probability density function.

We now turn our attention to assumptions on the distributions of these four quantities. While the quantities p, R, β , and r are likely interrelated, we assume that p, R, β , and r are independent to allow

simplifications and the following derivation. [Savransky et al. \(2011\)](#) showed that β is sinusoidally distributed regardless of the distribution of any other orbital parameter, dependent only on the second assumption above. All other parameters (a, e, p, R) are assumed to have probability density functions representative of the planet population of interest and are represented by random variables $(\bar{a}, \bar{e}, \bar{p}, \bar{R})$. Under the first three assumptions above and assuming independence between \bar{a} and \bar{e} , the probability density function for orbital radius ([Savransky et al. 2011](#)), $f_{\bar{r}}(r)$, is given by

$$f_{\bar{r}}(r) = \frac{1}{\pi} \int_0^\infty \int_0^1 \frac{r}{a \sqrt{(ae)^2 - (a-r)^2}} f_{\bar{e}}(e) de f_{\bar{a}}(a) da. \quad (5)$$

The limits of integration will be from the minimum to the maximum values of semimajor axis and eccentricity of the planet population of interest. Physically realizable solutions occur when the integrand is real, i.e., $(ae)^2 > (a-r)^2$.

3. DERIVATIONS

3.1. Completeness Joint Probability Density Function

The joint probability density function of the variables p, R, β , and r , given the assumptions from Section 2 is

$$f_{\bar{p}, \bar{R}, \bar{\beta}, \bar{r}}(p, R, \beta, r) = f_{\bar{p}}(p) f_{\bar{R}}(R) f_{\bar{\beta}}(\beta) f_{\bar{r}}(r). \quad (6)$$

The completeness joint probability density function, $f_{\bar{s}, \Delta \text{mag}}(s, \Delta \text{mag})$, will be found in two steps. We will perform a change of variables on Equation (6) ([Larson & Shubert 1979](#)) to get a joint probability density function of $s, \Delta \text{mag}, p$, and R , $f_{\bar{s}, \Delta \text{mag}, \bar{p}, \bar{R}}(s, \Delta \text{mag}, p, R)$. This distribution will then be marginalized to yield the completeness joint probability density function

$$f_{\bar{s}, \Delta \text{mag}}(s, \Delta \text{mag}) = \int_{-\infty}^{\infty} \int_{-\infty}^{\infty} f_{\bar{s}, \Delta \text{mag}, \bar{p}, \bar{R}}(s, \Delta \text{mag}, p, r) dR dp. \quad (7)$$

We begin by defining four new variables as functions of the original variables

$$s = g_1(p, R, \beta, r) = r \sin \beta \quad (8a)$$

$$\Delta \text{mag} = g_2(p, R, \beta, r) = -2.5 \log_{10} \left[p \left(\frac{R}{r} \right)^2 \Phi(\beta) \right] \quad (8b)$$

$$p = g_3(p, R, \beta, r) = p \quad (8c)$$

$$R = g_4(p, R, \beta, r) = R. \quad (8d)$$

All g_i are required to have continuous partial derivatives and $\Phi(\beta)$ must be differentiable since the inverse of the Jacobian determinant of Equation (8) will be used. All g_i satisfy this condition except for g_2 when any of the following occur: $p = 0, R = 0, \beta = 0, \pi$, and $r = 0$. At any of the values violating the condition of continuous partial derivatives, the joint probability density function, $f_{\bar{s}, \overline{\Delta \text{mag}}, \bar{p}, \bar{R}}(s, \Delta \text{mag}, p, R)$, is set to zero.

The Jacobian determinant of Equation (8) is given by

$$\begin{aligned} J(p, R, \beta, r) &= \begin{vmatrix} \frac{\partial g_1}{\partial p} & \frac{\partial g_1}{\partial R} & \frac{\partial g_1}{\partial \beta} & \frac{\partial g_1}{\partial r} \\ \frac{\partial g_2}{\partial p} & \frac{\partial g_2}{\partial R} & \frac{\partial g_2}{\partial \beta} & \frac{\partial g_2}{\partial r} \\ \frac{\partial g_3}{\partial p} & \frac{\partial g_3}{\partial R} & \frac{\partial g_3}{\partial \beta} & \frac{\partial g_3}{\partial r} \\ \frac{\partial g_4}{\partial p} & \frac{\partial g_4}{\partial R} & \frac{\partial g_4}{\partial \beta} & \frac{\partial g_4}{\partial r} \end{vmatrix} \\ &= \frac{-2.5}{\Phi(\beta) \ln 10} \Phi'(\beta) \sin \beta - \frac{5}{\ln 10} \cos \beta. \end{aligned} \quad (9)$$

$J(p, R, \beta, r)$ is required to be non-zero since its inverse will be used. This requirement is violated when $\beta = \beta^*$, where β^* maximizes $\sin^2 \beta \Phi(\beta)$ (Brown 2004a). As before, when $\beta = \beta^*$, the joint probability density function, $f_{\bar{s}, \overline{\Delta \text{mag}}, \bar{p}, \bar{R}}(s, \Delta \text{mag}, p, R)$, is set to zero.

We now define the inverse equations to Equation (8)

$$p = h_1(s, \Delta\text{mag}, p, R) = p \quad (10a)$$

$$R = h_2(s, \Delta\text{mag}, p, R) = R \quad (10b)$$

$$\beta = h_3(s, \Delta\text{mag}, p, R) \quad (10c)$$

$$r = h_4(s, \Delta\text{mag}, p, R) = \frac{s}{\sin(h_3(s, \Delta\text{mag}, p, R))} \quad (10d)$$

All of these equations must have a unique solution. h_3 and h_4 now pose a problem because they may have multiple solutions. Solutions to h_3 are the values of β which solve

$$\sin^2 \beta \Phi(\beta) = \frac{10^{-0.4\Delta\text{mag}} s^2}{pR^2}. \quad (11)$$

If h_3 has only one solution, $\beta = \beta^*$ and $f_{\bar{s}, \Delta\text{mag}, \bar{p}, \bar{R}}(s, \Delta\text{mag}, p, R) = 0$. If h_3 has no solution, $f_{\bar{s}, \Delta\text{mag}, \bar{p}, \bar{R}}(s, \Delta\text{mag}, p, R) = 0$. For the case of multiple solutions we use piecewise definitions for these equations. When two solutions occur, let β_1 and β_2 be the two solutions for h_3 and r_1 and r_2 be the corresponding solutions for h_4 :

$$\beta_1 = h_3(s, \Delta\text{mag}, p, R), \quad 0 < \beta_1 < \beta^* \quad (12a)$$

$$\beta_2 = h_3(s, \Delta\text{mag}, p, R), \quad \beta^* < \beta_2 < \pi \quad (12b)$$

and

$$r_1 = \begin{cases} \frac{s}{\sin \beta_1}, & r_{\min} \leq r_1 \leq r_{\max} \\ 0, & \text{else} \end{cases} \quad (13a)$$

$$r_2 = \begin{cases} \frac{s}{\sin \beta_2}, & r_{\min} \leq r_2 \leq r_{\max} \\ 0, & \text{else} \end{cases} \quad (13b)$$

where r_{\min} and r_{\max} are the minimum and maximum planet distances from the star. The joint

distribution function $f_{\bar{s}, \overline{\Delta_{\text{mag}}}, \bar{p}, \bar{R}}(s, \Delta_{\text{mag}}, p, R)$ is given by the sum of each piece,

$$\begin{aligned} f_{\bar{s}, \overline{\Delta_{\text{mag}}}, \bar{p}, \bar{R}}(s, \Delta_{\text{mag}}, p, R) &= f_{\bar{p}, \bar{R}, \bar{\beta}, \bar{r}}(h_1, h_2, \beta_1, r_1) |J(h_1, h_2, \beta_1, r_1)|^{-1} \\ &+ f_{\bar{p}, \bar{R}, \bar{\beta}, \bar{r}}(h_1, h_2, \beta_2, r_2) |J(h_1, h_2, \beta_2, r_2)|^{-1}. \end{aligned} \quad (14)$$

We now have expressions for all of the functions required in Equation (7).

3.2. Nonzero Regions of Completeness Joint Probability Density Function

For a given value of s , $f_{\bar{s}, \overline{\Delta_{\text{mag}}}}(s, \Delta_{\text{mag}})$ is only nonzero inside minimum and maximum values of Δ_{mag} . We now derive curves for minimum and maximum Δ_{mag} as a function of s and minimum and maximum values of the assumed planetary population parameters.

To find the minimum Δ_{mag} , we insert Equations (2) and (3) into Equation (4) to get

$$\Delta_{\text{mag}} = -2.5 \log_{10} \left[p \Phi(\beta) \left(\frac{R \sin \beta}{s} \right)^2 \right]. \quad (15)$$

Δ_{mag} is minimized when the expression inside the logarithm in Equation (15) is maximized. This leads to the obvious choices of p_{max} and R_{max} , the assumed planetary population parameters limits. To find the value of β , we find local extrema which are roots of the following equation (Brown 2004a):

$$2 \sin \beta \cos \beta \Phi(\beta) + \sin^2 \beta \frac{\partial \Phi(\beta)}{\partial \beta} = 0. \quad (16)$$

One root occurs for $\beta = \beta^*$ ($0 < \beta^* < \pi$). The other two roots at $\beta = 0$ and $\beta = \pi$ do not occur for all orbital orientations. The extrema for these orbital orientations occur at the planet's closest approach to the star in the plane of the sky, i.e., $\beta = \sin^{-1}(s/r)$ or $\beta = \pi - \sin^{-1}(s/r)$. The combination of β^* and s will give the minimum value of Equation (15) as long as $r_{\text{min}} \sin \beta^* \leq s \leq r_{\text{max}} \sin \beta^*$, where $r_{\text{min}} = a_{\text{min}}(1 - e_{\text{max}})$ and $r_{\text{max}} = a_{\text{max}}(1 + e_{\text{max}})$. Outside of this range, β must correspond to the

phase angle at the closest approach. Equation (17) summarizes these results.

$$\Delta\text{mag}_{\min}(s) = \begin{cases} -2.5 \log_{10} \left[p_{\max} \left(\frac{R_{\max}}{r_{\min}} \right)^2 \Phi \left(\sin^{-1} \left(\frac{s}{r_{\min}} \right) \right) \right] & 0 \leq s \leq r_{\min} \sin \beta^* \\ -2.5 \log_{10} \left[p_{\max} \left(\frac{R_{\max}}{s} \right)^2 \Phi(\beta^*) \right] & r_{\min} \sin \beta^* \leq s \leq r_{\max} \sin \beta^* \\ -2.5 \log_{10} \left[p_{\max} \left(\frac{R_{\max}}{r_{\max}} \right)^2 \Phi \left(\sin^{-1} \left(\frac{s}{r_{\max}} \right) \right) \right] & r_{\max} \sin \beta^* \leq s \leq r_{\max} \end{cases} \quad (17)$$

To find the maximum Δmag , we wish to minimize Equation (3). This leads to the obvious choices of assumed planetary population limits p_{\min} , R_{\min} , and r_{\max} . The value for β should give the smallest value of the phase function $\Phi(\beta)$. This occurs for $\beta = \pi - \sin^{-1}(s/r_{\max})$. Equation (18) gives this expression.

$$\Delta\text{mag}_{\max}(s) = -2.5 \log_{10} \left[p_{\min} \left(\frac{R_{\min}}{r_{\max}} \right)^2 \Phi \left(\pi - \sin^{-1} \left(\frac{s}{r_{\max}} \right) \right) \right] \quad (18)$$

4. VALIDATION OF DERIVED COMPLETENESS JOINT PROBABILITY DENSITY FUNCTION

As a check on the derived completeness joint probability density function, we performed a comparison of Monte Carlo trials to the functional approach derived here. The planetary population variables with their units, minimum and maximum values, and assumed probability density functions are summarized in Table 1. We assumed log-uniform distributions for semi-major axis, geometric albedo, and planetary radius as zeroth order approximations of the distributions of these quantities based on discovered exoplanets available in catalogs such as exoplanet.eu or exoplanets.org. The log-uniform distribution is given by:

$$f_{\bar{x}}(x) = \begin{cases} (x \ln [x_{\max}/x_{\min}])^{-1} & x \in [x_{\min}, x_{\max}] \\ 0 & \text{else.} \end{cases} \quad (19)$$

The second assumption in §2 requires the mean anomaly to have a uniform distribution. A uniform distribution is given by:

$$f_{\bar{x}}(x) = \begin{cases} (x_{\max} - x_{\min})^{-1} & x \in [x_{\min}, x_{\max}] \\ 0 & \text{else.} \end{cases} \quad (20)$$

By the second assumption in §2, β is sinusoidally distributed regardless of the distribution of any other orbital parameter (Savransky et al. 2011). The sinusoidal distribution is given by:

$$f_{\bar{x}}(x) = \begin{cases} \frac{\sin x}{2} & x \in [x_{\min}, x_{\max}] \\ 0 & \text{else.} \end{cases} \quad (21)$$

We assumed a Rayleigh distribution for eccentricity since it fits Kepler data well (Van Eylen & Albrecht 2015). The Rayleigh distribution is given by:

$$f_{\bar{x}}(x) = \begin{cases} \frac{x}{c\sigma^2} e^{-x^2/(2\sigma^2)} & x \in [x_{\min}, x_{\max}] \\ 0 & \text{else.} \end{cases} \quad (22)$$

where σ is a scale parameter and c normalizes such that the integral from x_{\min} to x_{\max} results in 1.

We also used the Lambert phase function,

$$\Phi_L(\beta) = \frac{1}{\pi} [\sin \beta + (\pi - \beta) \cos \beta]. \quad (23)$$

For the Monte Carlo trials, we generated one billion independent identically distributed (IID) samples of the planetary population variables according to their respective probability distributions. We calculated s and Δmag for each sample and determined the completeness joint probability density function after sorting the $(s, \Delta\text{mag})$ pairs into a 400×400 grid over the ranges $0 \leq s \leq 6.75$ and $10 \leq \Delta\text{mag} \leq 50$. These computations were performed in parallel on a 4-core 2.3 GHz processor taking ~ 20 minutes. Figure 1 shows the resulting completeness joint probability density function with the color log-scaled (base 10). Minimum and maximum Δmag (Equations (17) and (18)) are

Table 1. Planetary population distribution

Variable	Quantity	Unit	Minimum	Maximum	Distribution
a	semi-major axis	AU	0.5	5	log-uniform
e	eccentricity	\cdots	0	0.35	Rayleigh, $\sigma = 0.25$
M	mean anomaly	rad	0	2π	uniform
p	geometric albedo	\cdots	0.2	0.3	log-uniform
R	planetary radius	km	6,000	30,000	log-uniform
β	phase angle	rad	0	π	sinusoidal

shown. Even with one billion samples, the Monte Carlo trial method does not fill the space between the minimum and maximum Δmag values.

Using the same 400×400 grid over s and Δmag , we performed the calculations outlined in Section 3 at each point. These calculations were performed in parallel on the same 4-core 2.3 GHz processor taking ~ 80 minutes total. Each individual point on the grid took ~ 0.1 seconds on average to compute. We point out again that completeness requires integration over a region of this joint probability density function. The Monte Carlo approach takes the same amount of computational time whether one point or the entire grid is computed. If higher order numerical integration algorithms are used to compute the double integral giving completeness, the method derived here will give better accuracy and quicker computation times because relatively few functional evaluations are needed compared to fully sampling the space for the Monte Carlo approach. If during the calculation of single visit completeness for a list of 100 target stars by a numerical integration algorithm, the function is evaluated in parallel on the same 4-core 2.3 GHz processor on a 200×50 grid over s and Δmag (between the minimum possible Δmag and the maximum Δmag_0 for a population) it will take ~ 14

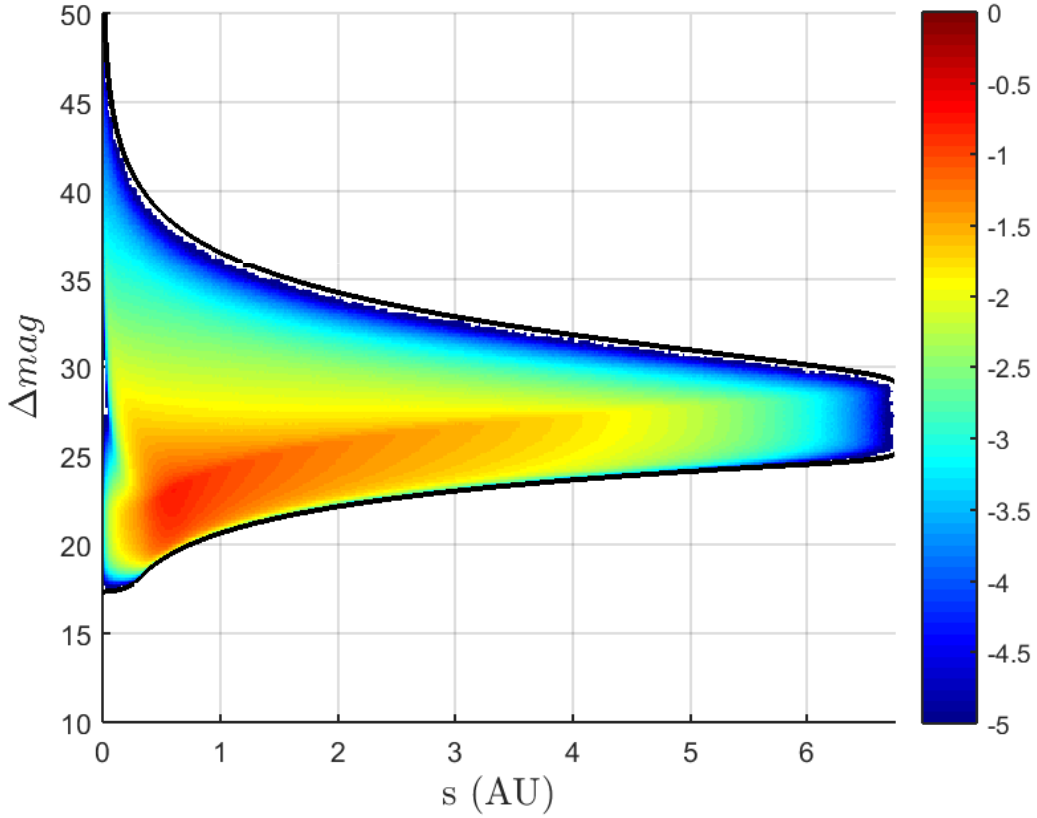


Figure 1. Completeness joint probability density function determined by one billion Monte Carlo trials. The color is log-scaled (base 10) of the probability density $\text{AU}^{-1}\Delta\text{mag}^{-1}$. The black lines represent minimum and maximum values for which the completeness joint probability density function is nonzero (given by Equations (17) and (18)). Blank space between these two lines shows that even with one billion trials the Monte Carlo approach does not adequately sample the entire s - Δmag phase space.

minutes. The functional completeness joint probability density function is shown in Figure 2 with the same color scale and minimum and maximum values of Δmag as in Figure 1. Visually, the two Figures look similar. The functional completeness joint probability density function shown in Figure 2, however, does not have the blank space that the Monte Carlo trial approach in Figure 1 has. This shows that the functional approach fills the s - Δmag phase space completely.

Figure 3 shows the absolute value of the percent difference of the Monte Carlo trials to the functional approach. We note agreement to better than 3% for the majority of the nonzero region of the s - Δmag plane. Larger discrepancies between the two methods occur near the minimum and maximum

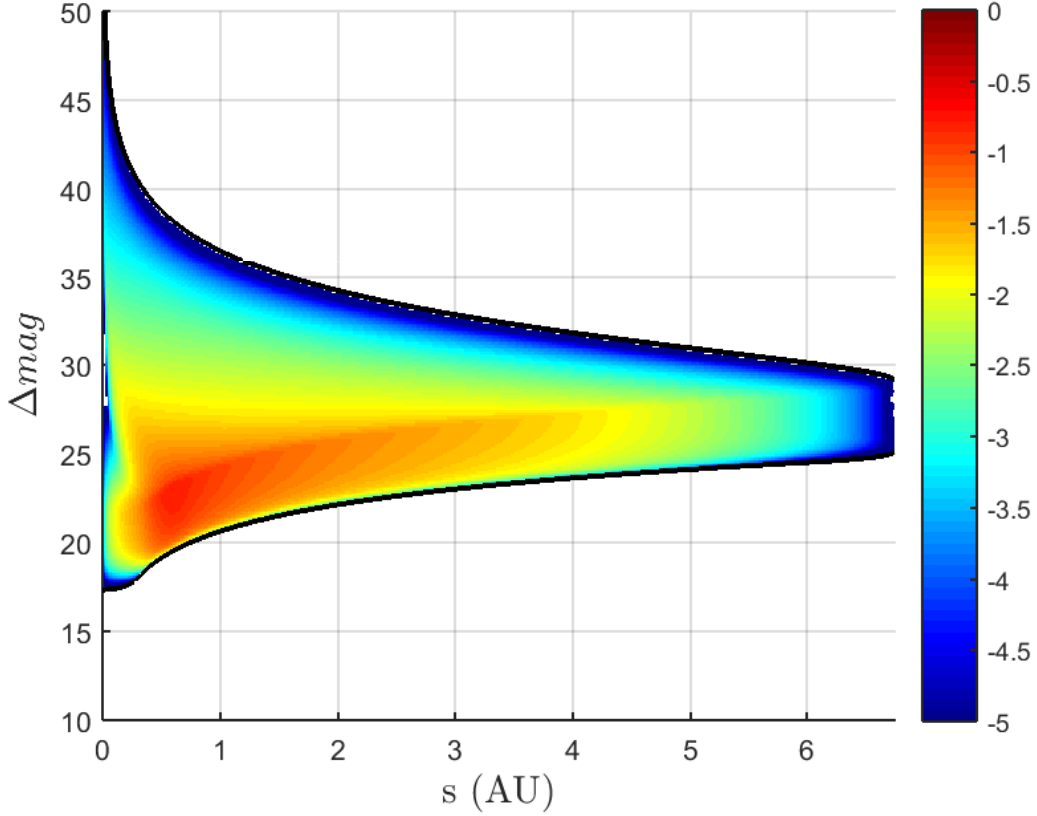


Figure 2. Completeness joint probability density function determined by functions in Section 3. The color is log-scaled in powers of 10 of the probability density $\text{AU}^{-1}\Delta\text{mag}^{-1}$. The black lines represent minimum and maximum values for which the completeness joint probability density function is nonzero (given by Equations (17) and (18)). There is no blank space between the lines showing that this approach fills the s - Δmag phase space.

boundaries where the Monte Carlo approach suffers from undersampling.

As further validation of the derivation, we performed the same one billion Monte Carlo trials and found probability density functions $f_{\bar{s}}(s)$ and $f_{\overline{\Delta\text{mag}}}(\Delta\text{mag})$. The functional approach determines these probability density functions by marginalizing the completeness joint probability density function as in Equations (24) and (25).

$$f_{\bar{s}}(s) = \int_{-\infty}^{\infty} f_{\bar{s}, \overline{\Delta\text{mag}}}(s, \Delta\text{mag}) d\Delta\text{mag} \quad (24)$$

$$f_{\overline{\Delta\text{mag}}}(\Delta\text{mag}) = \int_0^{\infty} f_{\bar{s}, \overline{\Delta\text{mag}}}(s, \Delta\text{mag}) ds \quad (25)$$

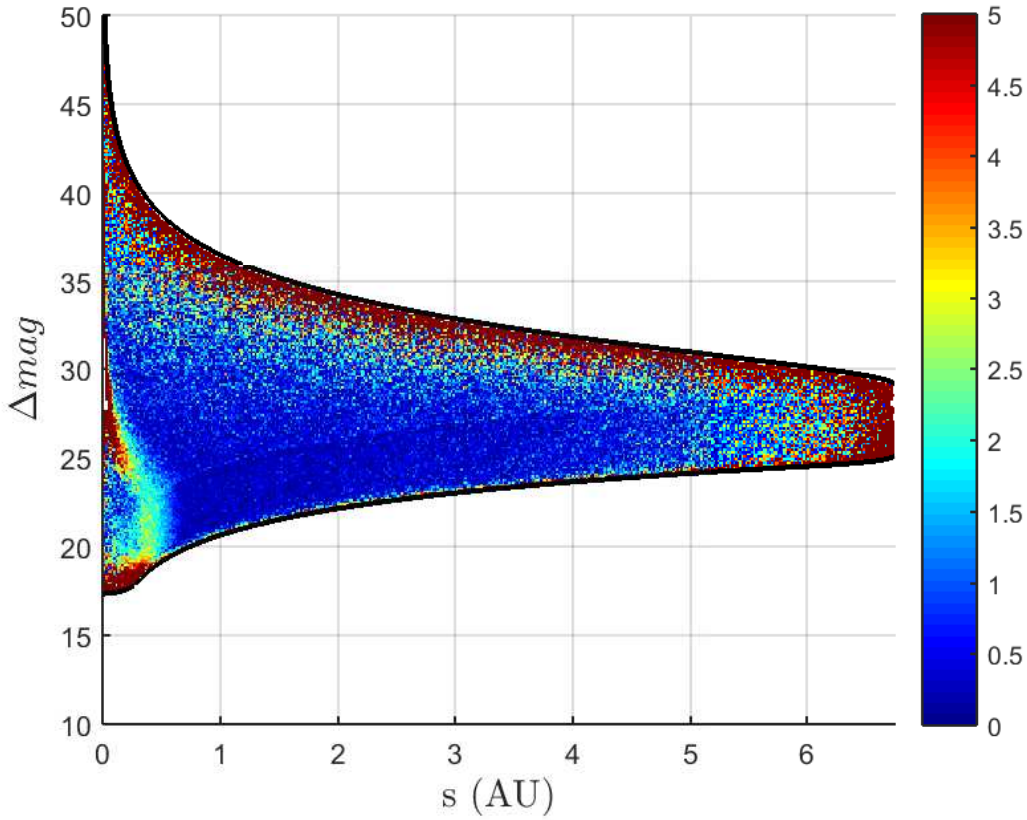


Figure 3. Absolute value of the percent difference from the Monte Carlo approach to the functional approach. The color is in percent. The black lines represent minimum and maximum values for which the completeness joint probability density function is nonzero (given by Equations (17) and (18)). Agreement between the two approaches is better than 3% for the majority of the s - Δmag plane. Large discrepancies occur where the Monte Carlo approach suffers from undersampling near the minimum and maximum Δmag values.

Figure 4 shows the comparison between the probability density function $f_{\bar{s}}(s)$ determined by the Monte Carlo approach and the functional approach. Figure 5 shows the comparison between the probability density function $f_{\overline{\Delta\text{mag}}}(\Delta\text{mag})$ determined by the Monte Carlo approach and the functional approach. For each of these probability density functions, the Monte Carlo and functional approaches show very good agreement.

5. CONCLUSIONS

We have derived an analytical approach for finding the completeness joint probability density function which avoids the undersampling inherent in Monte Carlo approaches and allows computation

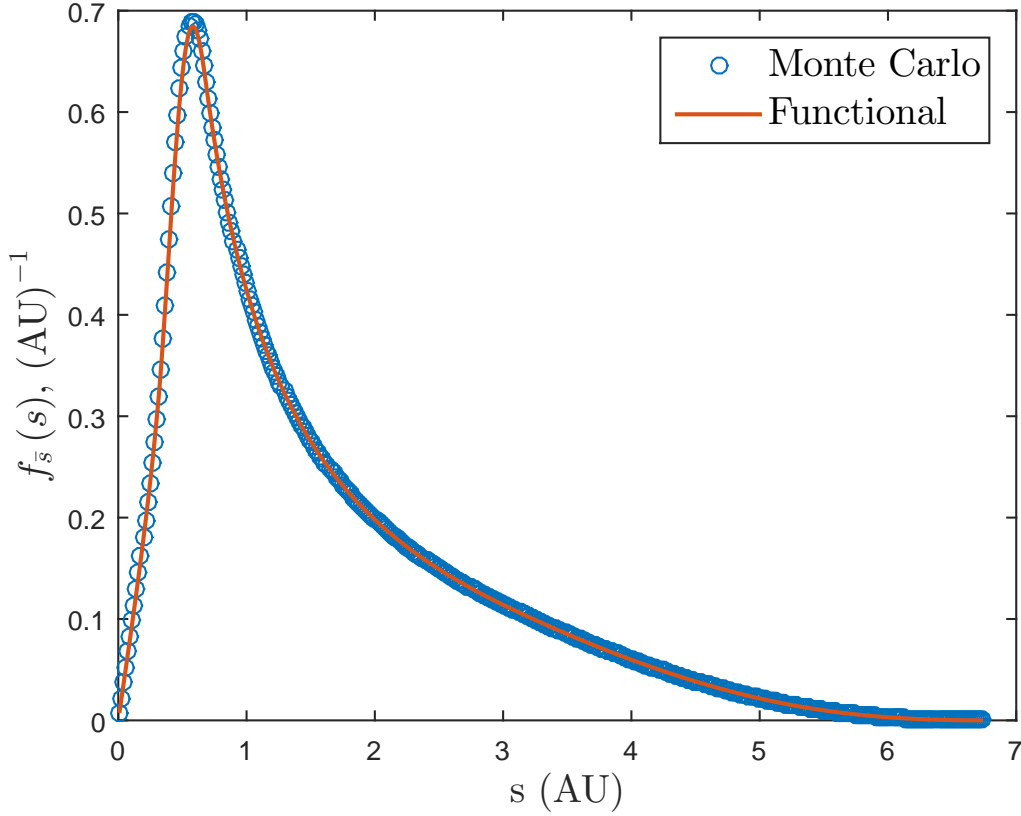


Figure 4. Comparison of Monte Carlo and functional approaches to determine $f_{\bar{s}}(s)$.

of a single point of this joint probability density function without simulation of the entire phase space. This allows a quicker, more accurate computation of the double integral giving completeness because the function is evaluated only at points necessary for computing the integral compared to sampling the entire parameter space fully with Monte Carlo trials. This approach is dependent on the assumptions of closed Keplerian orbits; orbital poles distributed uniformly over a spherical volume with respect to the observer; planet-planet interactions neglected; very large distance to target star; and independence of the distributions of geometric albedo, planetary radius, phase angle, and orbital radius. We have shown good agreement between this approach and the Monte Carlo approach. This approach will allow researchers more accurate computation of single-visit photometric and obscuration completeness, which will improve the estimate of the number of extrasolar planets

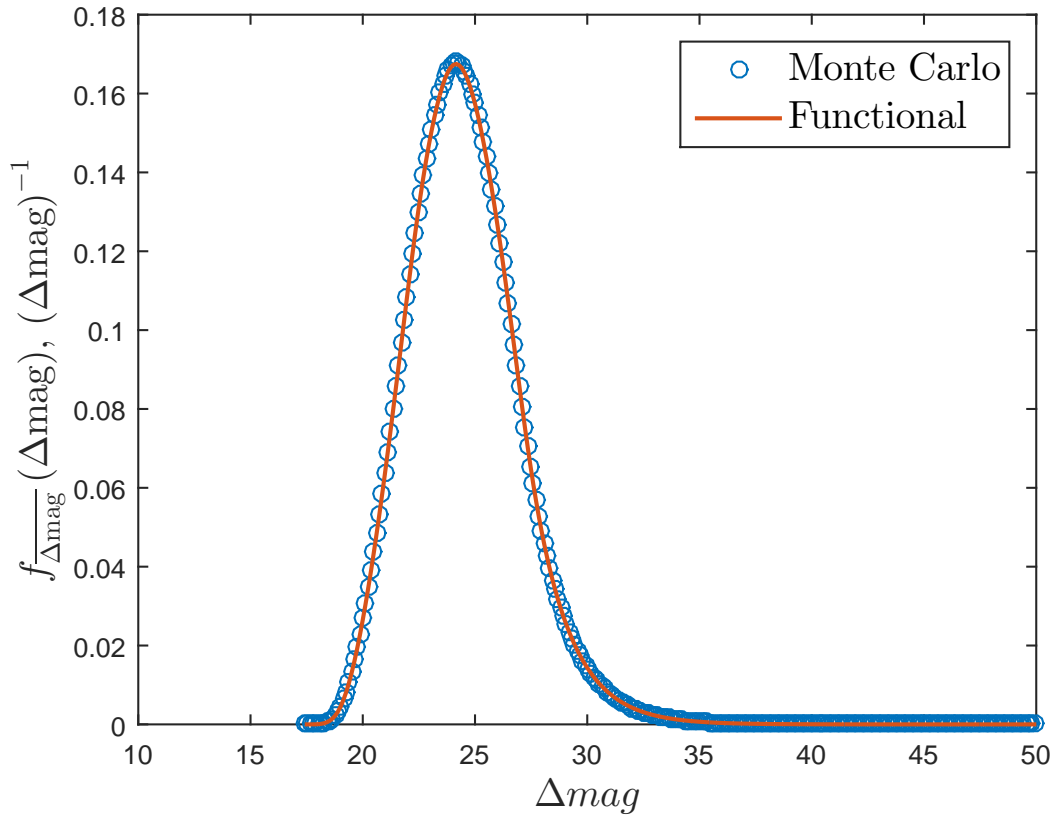


Figure 5. Comparison of Monte Carlo and functional approaches to determine $f_{\Delta \text{mag}}^{-1}(\Delta \text{mag})$.

discovered by direct-imaging planet-finding mission simulations and better inform mission design.

REFERENCES

- Agol, E. 2007, *Monthly Notices of the Royal Astronomical Society*, 374, 1271
- Brown, R. A. 2004a, *The Astrophysical Journal*, 610, 1079
- . 2004b, *The Astrophysical Journal*, 607, 1003
- . 2005, *The Astrophysical Journal*, 624, 1010
- . 2009a, *The Astrophysical Journal*, 699, 711
- . 2009b, *The Astrophysical Journal*, 702, 1237
- . 2015, *The Astrophysical Journal*, 799, 87
- Brown, R. A., & Soummer, R. 2010, *The Astrophysical Journal*, 715, 122
- Davis, P. J., & Rabinowitz, P. 2007, *Methods of numerical integration* (Courier Corporation)
- Larson, H. J., & Shubert, B. O. 1979, *Probabilistic models in engineering sciences*, Vol. 1 (Wiley)
- Lindler, D. J. 2007, in *Optical Engineering+ Applications*, International Society for Optics and Photonics, 668714–668714
- Savransky, D. 2013, in *SPIE Optical Engineering+ Applications*, International Society for Optics and Photonics, 886403–886403
- Savransky, D., Cady, E., & Kasdin, N. J. 2011, *The Astrophysical Journal*, 728, 66
- Savransky, D., & Kasdin, N. J. 2008, in *SPIE Astronomical Telescopes+ Instrumentation*, International Society for Optics and Photonics, 70101T–70101T
- Savransky, D., Kasdin, N. J., & Cady, E. 2010, *Publications of the Astronomical Society of the Pacific*, 122, 401
- Stark, C. C., Roberge, A., Mandell, A., et al. 2015, *The Astrophysical Journal*, 808, 149
- Stark, C. C., Roberge, A., Mandell, A., & Robinson, T. D. 2014, *The Astrophysical Journal*, 795, 122
- Van Eylen, V., & Albrecht, S. 2015, *The Astrophysical Journal*, 808, 126